Co-evolution Transformer for Protein Contact Prediction

Anonymous Author(s)
Affiliation
Address
email

Abstract

Proteins are the main machinery of life and protein functions are largely determined by their 3D structures. The measurement of the pairwise proximity between amino acids of a protein, known as inter-residue contact map, well characterizes the structural information of a protein. Protein contact prediction (PCP) is an essential building block of many protein structure-related applications. The prevalent approach to contact prediction is based on estimating the inter-residue contacts using hand-crafted coevolutionary features derived from multiple sequence alignments (MSAs). To mitigate the information loss caused by hand-crafted features, some recently proposed methods try to learn residue co-evolutions directly from MSAs. These methods generally derive coevolutionary features by aggregating the learned residue representations from individual sequences with equal weights, which is inconsistent with the premise that residue co-evolutions are a reflection of collective covariation patterns of numerous homologous proteins. Moreover, non-homologous residues and gaps commonly exist in MSAs. By aggregating features from all homologs equally, the non-homologous information may cause misestimation of the residue co-evolutions. To overcome these issues, we propose an attention-based architecture, Co-evolution Transformer (CoT), for PCP. CoT jointly considers the information from all homologous sequences in the MSA to better capture global coevolutionary patterns. To mitigate the influence of the non-homologous information, CoT selectively aggregates the features from different homologs by assigning smaller weights to non-homologous sequences or residue pairs. Extensive experiments on two rigorous benchmark datasets demonstrate the effectiveness of CoT. In particular, CoT achieves a 50.4% top-L long-range precision score for the Free Modeling (FM) domains on the CASP14 benchmark, which outperforms the winner group of CASP14 contact prediction challenge by 8.6%.

1 Introduction

Most *in vivo* biological processes are carried out by proteins, whose functions are mainly determined by their 3D structures [1]. Structural information is crucial for understanding the functions of a protein. The inter-residue contact map which measures the pairwise proximity between all amino acid pairs well characterizes the structural information of a protein. Protein contact prediction (PCP) is an important building block of many protein structure-related applications, such as protein structure prediction [2, 3], protein complex assembly [4], and protein design [5]. It is so important that it is one of the challenges of Critical Assessment of protein Structure Prediction (CASP), which is the "world championship" of the computational structural biology field.

The prevalent PCP approaches were built atop the co-evolution principle that the spatially proximate residues tend to co-evolve to maintain the functions of a protein [6–8]. The existing PCP methods

Submitted to 35th Conference on Neural Information Processing Systems (NeurIPS 2021). Do not distribute.

generally infer pairwise coevolutionary patterns from MSAs. Among them, direct coupling analysis (DCA) [9] techniques are widely used to obtain coevolutionary features by fitting Potts models or calculating precision matrix [10, 11]. Subsequently, a variety of deep-learning based methods were proposed to leverage the DCA-based features to estimate inter-residue contacts [3, 12–15]. However, DCA techniques only consider single-residue and pairwise statistics of the sequences, ignoring high-order interactions among the residues within a sequence.

To mitigate the information loss caused by hand-crafted features (e.g., DCA-based features), some recently proposed methods try to learn residue co-evolutions directly from MSAs [2, 16, 17]. For example, the SOTA of them, CopulaNet [2] learns residue representations from individual sequences and then aggregates these features with equal weights to derive residue co-evolutions. This causes two issues: 1) Inferring residue representations from individual sequences independently is inconsistent with the premise that residue co-evolutions are a reflection of collective covariation patterns of numerous homologs [18]; 2) Assigning equal weights to the features coming from different homologs ignores the fact that, the quality of homologs varies a lot because of the existence of non-homologous residues and gaps [19, 20].

In this paper, we propose an attention-based architecture, Co-evolution Transformer (CoT), to address or mitigate the issues discussed above. The core component of CoT is the *co-evolution attention* (CoA) module. Different from the previous methods that focus on extracting information from individual sequences, CoA is capable of incorporating the residue co-evolution patterns derived from all homologous sequences into an attention function to learn residue representations. Moreover, the CoA learns to automatically weight the residue representations learned from different homologs, and then selectively aggregates the features to construct the co-evolution attention map. This design mitigates the influence of non-homologous information.

CoT dramatically outperforms the baseline methods on two rigorous benchmarks CASP14 [21] and CAMEO (Continuous Automated Model EvaluatiOn) [22]. In particular, CoT achieves a 50.4% top-L long-range precision score for the Free Modeling (FM) domains on the CASP14 benchmark, which outperforms the winner group of CASP14 contact prediction challenge by 8.6%.

2 Related Work

Protein contact prediction is a binary classification task for amino acid residue pairs. A residue pair is called a contact if their distance is less than or equal to a distance threshold, typically 8Å, i.e., $8 \times 10^{-10}\mathbf{m}$.

As widely acknowledged, co-evolution information is closely correlated to the contacts. In order to extract the co-evolution patterns for residue pairs, multiple sequence alignments (MSAs) are generated from raw protein sequences. For a target protein sequence, a generated alignment consists of multiple sequences with each corresponding position being an aligned residue or a gap (annotated by a dash), and these aligned sequences as a whole are called a multiple sequence alignment. Many protein databases as well as various search schemes have been proposed to generate MSAs efficiently [19, 20]. There are roughly three categories of methods for predicting contacts from MSAs, namely, unsupervised methods, supervised methods, and pre-training based methods.

Unsupervised Methods To quantify the strength of the direct relation between the residue pairs of a protein sequence while excluding effects from other residues, many statistical modeling methods based on direct coupling analysis (DCA) have been proposed to fit Potts models [10] or precision matrix [11] to MSAs, e.g., mean-field DCA [9], sparse inverse covariance [11] and pseudo-likelihood maximization [10, 23, 24], to name a few. These methods further exploit dedicated scores based on DCA for contact prediction. However, they only consider single-residue and pairwise statistics of the sequences, thus fail to capture high-order interactions among the multiple residues within a sequence.

Supervised Methods By taking DCA-derived scores as features, deep neural networks based supervised methods significantly outperform the unsupervised methods [3, 12–15]. However, the information lost by the DCA-based features from the sequences is still not recoverable. To mitigate this issue, several models are proposed to learn residue co-evolution information directly from the sequences in the MSAs [2, 16, 17, 25]. Among them, CopulaNet [2], the SOTA of the CASP13 benchmark, derives coevolutionary features differentially by aggregating the learned residue rep-

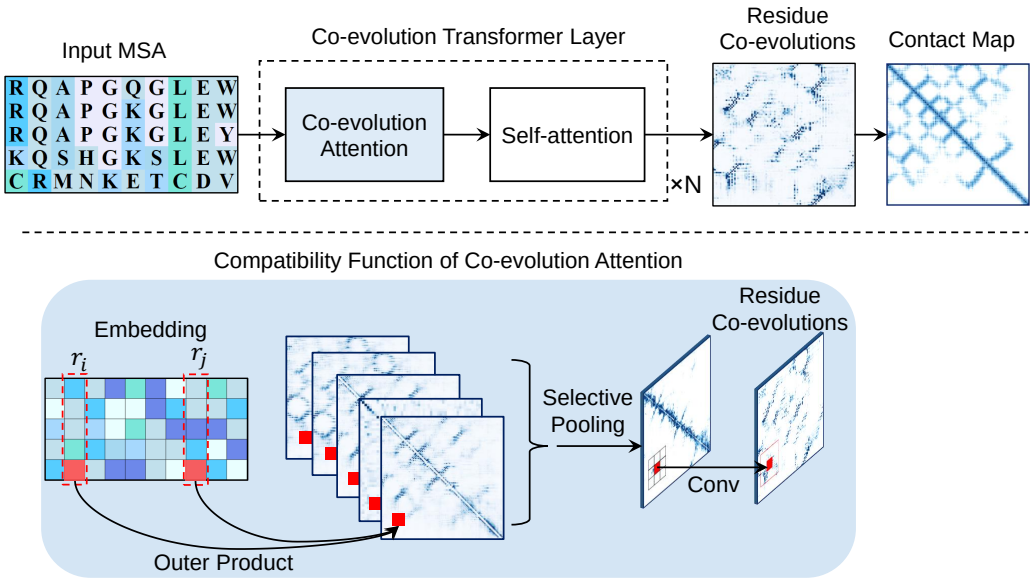

Figure 1: An Overview of Co-evolution Transformer. Given an input MSA, several CoT layers are stacked to learn residue representations, which are then used to derive residue co-evolutions to estimate inter-residue contacts. Each CoT layer consists of a co-evolution Attention (CoA) module and a self-attention module.

resentations from the sequences. However, although they are capable of modeling the high-order interactions among the multiple residues within single sequence, the global information carried by the MSAs is ignored because they still model the protein sequences independently. AlphaFold2 [25] is claimed to be modeling the full MSAs, achieving an amazing performance on the CASP14 structure prediction task. Although its performance on the structure prediction task is remarkable, they did not participate in the CASP14 PCP task meanwhile no further details of their methods are publicly available.

Pre-training Based Methods Following the *pre-train and fine-tune* paradigm, pre-trained language models are adapted to representation learning for protein sequences from the unlabeled data [26–31]. Many of them take contact prediction as an important downstream task to validate their performance. While these methods show another solution to this task, they are still at an early stage thus cannot achieve comparable performance to the SOTA approaches currently. To further improve the performance, a pre-trained language model named MSA Transformer is proposed to learn a better MSA representation directly [29]. This model shows the possibility of modeling the co-evolution information from MSAs, but it still cannot well extract the co-evolution information due to the non-homologous subsequences inevitably introduced by the generated MSAs.

To exploit the co-evolution information from the full MSAs effectively, our proposed CoT model is built upon *co-evolution attention*, a novel attention mechanism dedicated to incorporate the co-evolution information directly from MSAs.

3 Co-evolution Transformer

Co-evolution Transformer (CoT) is constructed by stacking several repeated CoT layers. Each CoT layer is composed of two attention modules, i.e., a *co-evolution attention* (CoA) module and a *self-attention* module, as shown in Figure 1. Given a prepared MSA, the stacked CoT layers are used to learn the residue representations. Residue co-evolutions are derived from the representations of the final layer and further employed to estimate the inter-residue contacts.

In this section, we first start with a brief introduction to the vanilla Transformer Encoder, followed by the detailed descriptions of each CoT component. To better illustrate the co-evolution attention

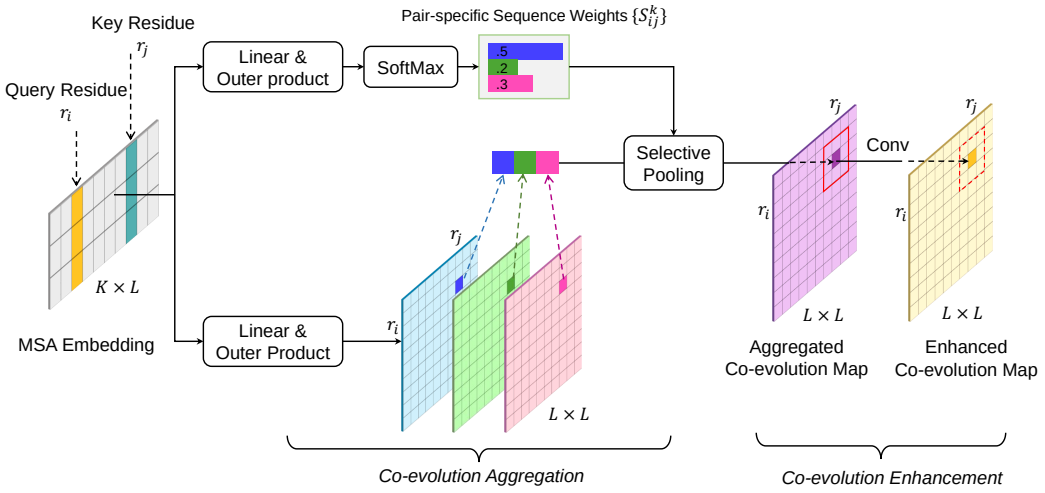

Figure 2: Schema of Co-evolution Attention. Given a residue pair $\langle r_i,\ r_j \rangle$, we first learn K covariance features and a set of pair-specific sequence weights S_{ij}^k, $k = 1 \cdots K$. The weights are used to selectively aggregate the K features. Finally, the aggregated feature is fed to a convolutional module to obtain the co-evolution attention map. For better visualization, we omit the feature channels and the details about how co-evolution attention attend to residue embeddings.

mechanism, the proposed co-evolution attention mechanism and the self-attention mechanism are discussed in the end.

3.1 Vanilla Transformer Encoder

Transformer is a network architecture built on the self-attention mechanism for machine translation. The Transformer encoder is widely adopted for machine learning tasks due to its excellent feature extraction capability when modeling long-distance interactions in sequences [32–34]. Each Transformer encoder layer consists of two modules, i.e., a *multi-head self-attention* (MHSA) module and a *position-wise fully connected feed-forward* (FFN) module. To connect these two modules, residual connections [35] and layer normalization (LayerNorm) [36] are applied as below:

$$x = \text{LayerNorm}(x + \text{MHSA}(x)), \tag{1}$$
$$x = \text{LayerNorm}(x + \text{FFN}(x)), \tag{2}$$

The multi-head self-attention module is also adopted by the CoT layer as a component to learn the residue representations of different sequences in the MSA, however, iterating through the columns instead of rows/sequences.

3.2 Co-evolution Attention Module

To extract co-evolution information from both inter- and intra- sequences in the MSA as well as to deal with the non-homologous information for the target sequence, a CoA module employs two consequent submodules, i.e. *co-evolution aggregation* and *co-evolution enhancement*, to the multi-head co-evolution attention from the MSA. The co-evolution aggregation submodule is designed to generate the coevolutionary features by aggregating pairwise interactions from all homologs in the MSA, while the co-evolution enhancement submodule further enhances the coevolutionary features and derives the final co-evolution attention. The overview of the CoA module is illustrated in Figure 2.

Given a target protein sequence $(r_1, r_2 \ldots r_L)$ and its MSA, where L is the length of the sequence, the corresponding representation is denoted as $X \in \mathbb{R}^{K \times L \times d_{model}}$, where K is the number of homologous sequences and d_{model} is the hidden dimension of the residue representation.

For the k-th sequence in the MSA, the overall procedure of the CoA module in each layer can be summarized as follows:

$$X^k = \textsc{LayerNorm}(X^k + \textsc{CoAttn}(X)), \tag{3}$$

$$X^k = \textsc{LayerNorm}(X^k + \text{FFN}(X^k)) \tag{4}$$

where $k \in [1 \dots K]$ and $\textsc{CoAttn}$ is defined as:

$$\textsc{CoAttn}(X) = \textsc{Concat}(\text{head}_1, \dots, \text{head}_H), \tag{5}$$

$$\text{head}_h = \textsc{Attn}_h(X,\ A)\, X_h^k\, W_h, \tag{6}$$

where $h \in [1 \dots H]$ is the head index, $A \in \mathbb{R}^{L \times L \times d_{co}}$ is the co-evolution feature map generated with d_{co} as its feature dimension, $\textsc{Attn}_h(X,\ A) \in \mathbb{R}^{L \times L}$ is the h-th co-evolution attention head, $X_h^k \in \mathbb{R}^{L \times d_v}$ is the h-th segment of X^k, and $W_h \in \mathbb{R}^{d_v \times d_v}$ are learnable weights ($d_v = d_{model}/H$). Note that the co-evolution attention $\textsc{Attn}_h(X,\ A)$ is shared by all the K homologous sequences within the same head.

Submodule 1: Co-evolution Aggregation To depict inter-residue interactions, the co-evolution aggregation submodule exploits outer product on the residue representations. A selective pooling operation is then applied to the aggregated outer products from all homologous sequences, the disturbance of non-homologous information can be greatly reduced by this weighting mechanism.

Two tensors $P,\ Q \in \mathbf{R}^{K \times L \times d_{model}}$, are generated from X by separate linear projections. For the residue pair $\langle r_i, r_j \rangle$ in the k-th sequence of the MSA, the pair co-evolution features A_{ij} are calculated by:

$$A_{ij} = \textsc{Proj}\left(\sum_{k=1}^{K} S_{ij}^k \odot (P_i^k \otimes P_j^k)\right), \tag{7}$$

and

$$S_{ij}^k = \frac{1}{Z} \exp(Q_i^k \otimes Q_j^k), \tag{8}$$

where $\otimes$ is the outer product operator, $\odot$ is the element-wise multiplication operator, $\textsc{Proj}$ is a flatten operation followed by a linear projection, converting the aggregated pair co-evolution features to $A \in \mathbb{R}^{L \times L \times d_{co}}$, and Z stands for the normalization factor. The weight for the pair representation is denoted as S_{ij}^k, where $S_{ij}^k \in \mathbb{R}^{d_{model} \times d_{model}}$ whose elements fall in the range of $[0, 1]$. The weights are normalized over the k sequences, thus we have $\sum_k S_{ij}^k = \mathbf{1}$.

Submodule 2: Co-evolution Enhancement To model the high-order interactions among multiple residues, the co-evolution map A is concatenated with A' from the previous CoT layer, the values are fed into a convolutional module ($\textsc{Conv}$) to generate an enhanced co-evolution map by:

$$A = \textsc{Conv}([A'; A]). \tag{9}$$

The h-th co-evolution attention head is projected from A by

$$\textsc{Attn}_h(X,\ A) = \textsc{SoftMax}(A\, M_h), \tag{10}$$

where $M_h \in \mathbb{R}^{d_{co} \times 1}$ are learnable weights.

3.3 Why Co-evolution Attention

A straightforward way to model the co-evolution is by applying self-attention to individual sequences in the MSA. In this case, for a residue pair $\langle r_i,\ r_j \rangle$ in the k-th homolog, self-attention measures their compatibility (attention weight, $\mathcal{A}_{ij}^k$) by:

$$\mathcal{A}_{ij}^k \propto \textsc{SoftMax}\{(U X_i^k)^\top (V X_j^k)\}, \tag{11}$$

where U, V are learnable weights.

In comparison, the attention weight of CoA, calculated by the co-evolution aggregation module (AGGREGATE) and the co-evolution enhancement module (ENHANCE), can be summarized as:

$$A_{ij} = \text{AGGREGATE}(X_i \otimes X_j), \tag{12}$$

$$A_{ij} = \text{ENHANCE}(A_{ij}, \text{NEIGHBOR}(i, j)), \tag{13}$$

$$\mathcal{A}_{ij}^{k} \propto \text{SOFTMAX}\{A_{ij}\}, \tag{14}$$

Compare with self-attention, co-evolution attention is more expressive at three aspects: 1) CoA leverages the global information from all the homologs instead of single homolog to derive the attention, which fits better to the residue co-evolution insight; 2) CoA handles the non-homologous information naturally by the selective pooling operation during aggregation, providing a solution to a widely existed but inevitable dilemma for MSAs; 3) CoA enhances the co-evolution signal by propagating information from the neighbors, making it easier to capture the high-order interactions among multiple residues.

4 Experimental Evaluation

We have conducted extensive experiments and analyses to evaluate the effectiveness of CoT.

4.1 Experiment Setup

Benchmark. Two standard benchmarks are used for the model evaluation in the conducted experiments, i.e., CASP14 and CAMEO. 1) CASP14 is the latest and most important benchmark for protein contact prediction [21]. This benchmark includes three kinds of protein domains, i.e., FM (22 domains), FM/TBM (14 domains), and TBM (50 domains), where a domain is a protein sequence prepared by the CASP organizers. The first protein among them was released on May. 18, 2020. 2) CAMEO is another benchmark to evaluate weekly-updated protein structure submissions continuously [22]. The proteins are classified into three categories: easy, medium, and hard. Among them, 176 hard targets, released in the last year (from 2020-04-17 to 2021-04-10), are selected for model evaluation.

Dataset. All models are trained on $96,167$ protein structures (chains) collected from PDB [37] (before Apr. 1, 2020). The proteins in PDB from Apr. 1, 2020 to Dec. 25, 2020 are used as the validation set for hyperparameter search. For each protein sequence, we generate its MSA by searching UniRef30 (version 2020-02), UniRef90 (version 2020-02), BFD30 (version 2019-03), MGnify90 (version 2019-05) with HHblits (version 3.3.0) and HMMER (version 3.3.2). The details of the MSA generation procedure are described in Appendix.

Evaluation. Following the procedure of trRosetta [15], the contact prediction task is converted into a multi-class classification task. The inter-residue distance range is divided into 37 bins, i.e., $(0\,\text{Å}, 2.5\,\text{Å}], (2.5\,\text{Å}, 3.0\,\text{Å}], \cdots, (20.0\,\text{Å}, +\infty)$, while the models are trained with the bin labels. For contact, the summed probability value of the bins with distance less than $8\,\text{Å}$ are used as the final prediction.

Metrics. For the evaluation criterion, the prevalent metrics are employed, which are *Precision*$@L$, *Precision*$@L/2$, and *Precision*$@L/5$ of long-range residue contacts, where *Precision*$@n$ stands for the precision score for the most confident n predictions. Here, L refers to the length of protein sequence and *long-range* means there are at least 23 other residues between these two residues in the sequence.

Implementations. Given an MSA, 256 sequences are randomly sampled and cropped by length 200. The CoT model is equipped with 6 CoT layers with hidden size as 128 and the attention head number as 8. All models are trained with Adam optimizer [38] via a cross-entropy loss for $100k$ iterations. The learning rate, the weight decay, and the batch size are set to 10^{-4}, 0.01, and 16 respectively. The hyperparameter details are listed in Appendix. The total training cost of the CoT model is about 30 hours on 4 Tesla V100 GPU cards.

4.2 Evaluation Results

For the sake of fairness, CoT is compared with three SOTA methods for contact prediction, including RaptorX [14], trRosetta [15] and CopulaNet [2], on the identical MSAs by searching BFD30 using

Table 1: Comparison on CASP14 and CAMEO (*Precision@L*)

Methods	CASP14			CAMEO
	FM (22)	FM/TBM (14)	TBM (50)	Hard (176)
RaptorX [14]	33.9	58.1	63.1	53.2
trRosetta [15]	31.3	57.6	61.1	50.1
CopulaNet [2]	38.5	62.2	65.5	56.5
CoT-SA (ours)	41.8	59.2	67.9	59.8
CoT (ours)	**47.5**	**63.0**	**76.1**	**66.4**

Table 2: Comparison on CASP14. Gr. 368, Gr. 488, and Gr. 010 are the results of the top-3 groups in the CASP14 challenge. CoT† refers to the results of CoT with MSA selection.

Method	FM (22)			FM/TBM (14)			TBM (50)		
	L	$L/2$	$L/5$	L	$L/2$	$L/5$	L	$L/2$	$L/5$
Gr. 368	41.8	55.7	66.6	64.5	78.6	87.4	73.1	87.1	94.5
Gr. 488	40.4	52.9	65.0	63.6	78.8	88.5	72.0	86.9	93.7
Gr. 010	39.6	53.4	63.8	61.5	77.0	86.8	66.1	80.9	89.5
CoT† (ours)	**50.4**	**65.5**	**76.0**	**66.7**	**81.5**	**90.6**	**78.9**	**92.0**	**98.2**

HHblits with default parameters. As shown in Table 1, CoT outperforms the baselines, while surpassing CopulaNet, the best of the SOTAs, by 9.0%, 0.8%, 10.6% and 9.9% for *Precision@L* scores on four kinds of targets, respectively. The improvement on FM/TBM domains (0.8%) is not that significant as the others ($> 9.0\%$), and a possible reason is that the performance varies a lot on the small number of domains.

Methods used by the groups participated in the CASP14 challenge are considered to the best for the benchmark due to their deep optimization towards MSA generation and model ensemble strategy. To further evaluate the performance of the proposed method, the top-3 winner groups/methods on CASP14 are compared with CoT. Different groups use different data sources to build their MSAs. To eliminate the variance of different data sources, the most confident prediction of CoT on 12 MSAs from different databases with different search settings, denoted as CoT†, is selected as the final prediction.

As shown in Table 2, CoT† outperforms the best method. On the hardest domains (CASP14-FM), CoT† even increases 8.6%, 9.9%, 9.4% scores for all the three metrics, compared with Gr. 368, the best group on this benchmark.

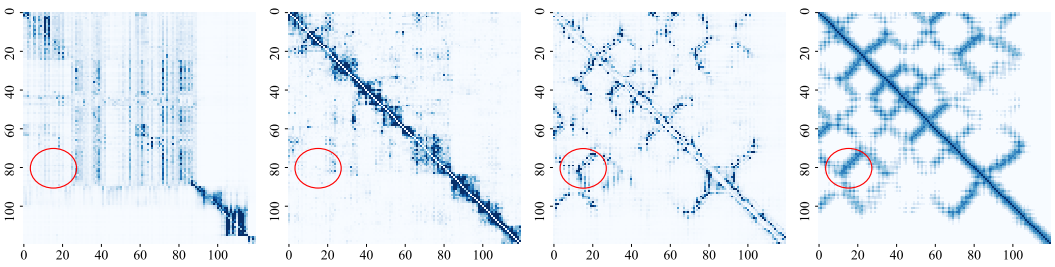

Figure 3: Comparison of the extracted attention maps for `4q2z_H`. (a) CoT-SA model; (b) CoT model w/o co-evolution enhancement; (c) CoT model; (d) Ground-truth contact map. The red circle covers typical long-range contacts.

Table 3: Ablations for CoA on CASP14 (*Precision@L*). AGGRE., ENHAN. and SA refer to the co-evolution aggregation submodule, the co-evolution enhancement submodule, and the self-attention module, respectively.

			CASP14			CAMEO
AGGRE.	ENHAN.	SA	FM (22)	FM/TBM (14)	TBM (50)	Hard (176)
Selective Pooling	✓	✓	47.5	63.0	76.1	66.4
Average Pooling	✓	✓	42.7	62.2	73.6	64.2
Selective Pooling		✓	41.6	61.2	70.3	61.8
Selective Pooling	✓		46.4	66.9	74.8	66.3

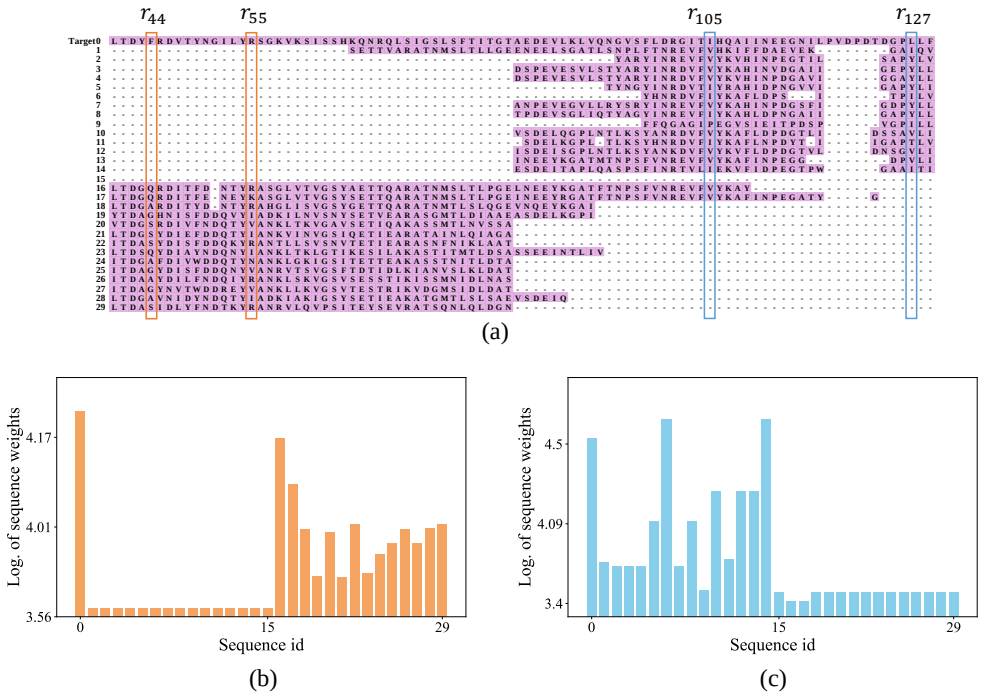

Figure 4: Learned sequence weights for `T1061-D1`. (a) Part of MSA for `T1061-D1` (residue 40-130), where the purple region represents aligned residues and '-' stands for a gap. (b) The sequence weight distribution for the pair $\langle r_{44}, r_{55} \rangle$. (c) The sequence weight distribution for the pair $\langle r_{105}, r_{127} \rangle$.

4.3 Comparison with Self-attention

To compare co-evolution attention with self-attention, a CoT model variant where the CoA module is replaced by the self-attention module is implemented (denoted as CoT-SA). Both CoT and CoT-SA are evaluated on the CASP14 and CAMEO benchmarks. As shown in Table 1, the CoT outperforms CoT-SA by 5.7%, 3.8%, 8.2%, and 6.6% Precision@L scores on four kinds of targets, indicating that CoA is much better than self-attention for this task. To further understand the co-evolution attention, the two attention matrices for both models are visualized. As shown in Figure 3 (a) and (c), the co-evolution attention patterns are much closer to the ground-truth contact map than that of self-attention, illustrating that CoA is more effective in extracting contact patterns.

4.4 Ablation Study

To evaluate the contribution of each model component, we set up ablative configurations for the co-evolution aggregation submodule, the enhancement submodule, and the self-attention module.

Experiments with various ablative configurations are conducted as listed in Table 3. For the co-evolution aggregation submodule, an *average pooling* is implemented as an alternative of *selective pooling*, where the features of different sequences are aggregated equally. The result shows that selective pooling obviously plays a critical role in the model, as the *Precision*@L score of the models with selective pooling on FM domains increased from 42.7% to 47.5% compared with that with average pooling.

Figure 4 (a) is an MSA for the CASP14 target `T1061-D1`. Since the model is not sensitive to MSA sequence order, we rearrange the MSA for better visualization. Then we visualize the sequence weights CoT learned from the MSA for two selected residue pairs $\langle r_{44}, r_{55} \rangle$ and $\langle r_{105}, r_{127} \rangle$. Figure 4 (b) and (c) show that selective pooling assigns larger weights to more relevant sequences as expected. Meanwhile, the difference between two sequence weight distributions of the two pairs demonstrates that the model is able to learn pair-specific weights.

The *co-evolution enhancement* is a convolutional module to learn correlations among multiple residues, and the overall performance reduces significantly on FM domains from 47.5% to 41.6% when removing this module, as compared in Table 3. These results illustrate that the high-order residue interaction is very important for contact prediction, as the interaction might reflect some structure patterns (e.g, structure motifs) [14, 39]. Moreover, as illustrated in Figure 3, by applying co-evolution enhancement, long-range residue interactions can be better extracted.

By ablating the self-attention module, the overall model performance drops slightly, indicating that the CoA module is the main contributor to achieve the performance.

4.5 Model Analysis

The Effect of MSA Quality The quality of predicted contacts is highly related to M_{eff} [40], which is the number of the non-redundant sequence homologs in the MSA (sequences of more than 70% identity is considered redundant). For the CASP14 FM domains, the correlation coefficients between the logarithm of M_{eff} and the *Precision*@L scores is 0.68, demonstrating that the performance of contact prediction is strongly correlated to MSA quality. CoT cannot predict the contact maps of some proteins very well (e.g., the *Precision*@L score of `T1093-D1` is only 13.5%). For most of these proteins, the M_{eff} is as small as less than 20, indicating that low-quality MSAs are still a bottleneck for contact prediction.

The Effect of Training Data To the best of our knowledge, there is no unified MSA generation pipeline for PCP and most state-of-the-art models are trained on their private training data, which are usually unavailable. To study the effect of training data, we train another model CoT* on a smaller training dataset but of comparable size to that used by CopulaNet [2], i.e., PDB30. The performance of CoT* is slightly lower than CoT, e.g., 46.3% vs. 47.5% for *Precision*@L on the CASP14 FM domains and 66.1% vs. 66.4% on the CAMEO hard targets. But it still outperforms CopulaNet a lot, for example, 46.3% vs. 38.2% for *Precision*@L on CASP14 FM domains. These results demonstrate that the performance gain of CoT is not mainly achieved by the larger size of the training data.

For the other hyperparameters for CoT, the empirical results are summarized in Appendix.

5 Conclusions

We propose an attention-based architecture (CoT) to learn residue coevolutions from multiple sequence alignments (MSAs). As the core component of CoT, co-evolution attention (CoA) leverages the full information of an MSA to learn residue representations by treating coevolutionary patterns as attention. Moreover, it employs a selective pooling operation to mitigate the influence of non-homologous information. The experimental results on two rigorous benchmarks demonstrate the effectiveness of CoT.

On the other hand, the experimental results also reveal a failure case of CoT, i.e., CoT cannot accurately predict the contacts of proteins with low-depth MSAs. This is an issue shared by other existing approaches as well. How to address the issue caused by low-quality MSAs remains an open problem. We believe pretrained protein models may be a potential solution to it [26–30].

References

[1] David Whitford. *Proteins: structure and function*. John Wiley & Sons, 2013.

[2] Fusong Ju, Jianwei Zhu, Bin Shao, Lupeng Kong, Tie-Yan Liu, Wei-Mou Zheng, and Dongbo Bu. CopulaNet: Learning residue co-evolution directly from multiple sequence alignment for protein structure prediction. *Nature Communications*, 12(1):1–9, 2021.

[3] Andrew W Senior, Richard Evans, John Jumper, James Kirkpatrick, Laurent Sifre, Tim Green, Chongli Qin, Augustin Žídek, Alexander WR Nelson, Alex Bridgland, et al. Improved protein structure prediction using potentials from deep learning. *Nature*, 577(7792):706–710, 2020.

[4] Yumeng Yan and Sheng-You Huang. Accurate prediction of inter-protein residue–residue contacts for homo-oligomeric protein complexes. *Briefings in Bioinformatics*, 2021.

[5] Ivan Anishchenko, Tamuka Martin Chidyausiku, Sergey Ovchinnikov, Samuel J Pellock, and David Baker. De novo protein design by deep network hallucination. *bioRxiv*, 2020.

[6] Thomas A Hopf, Lucy J Colwell, Robert Sheridan, Burkhard Rost, Chris Sander, and Debora S Marks. Three-dimensional structures of membrane proteins from genomic sequencing. *Cell*, 149(7):1607–1621, 2012.

[7] Debora S Marks, Thomas A Hopf, and Chris Sander. Protein structure prediction from sequence variation. *Nature biotechnology*, 30(11):1072–1080, 2012.

[8] Qi Wu, Zhenling Peng, Ivan Anishchenko, Qian Cong, David Baker, and Jianyi Yang. Protein contact prediction using metagenome sequence data and residual neural networks. *Bioinformatics*, 36(1):41–48, 2020.

[9] Faruck Morcos, Andrea Pagnani, Bryan Lunt, Arianna Bertolino, Debora S Marks, Chris Sander, Riccardo Zecchina, José N Onuchic, Terence Hwa, and Martin Weigt. Direct-coupling analysis of residue coevolution captures native contacts across many protein families. *Proceedings of the National Academy of Sciences*, 108(49):E1293–E1301, 2011.

[10] Magnus Ekeberg, Cecilia Lövkvist, Yueheng Lan, Martin Weigt, and Erik Aurell. Improved contact prediction in proteins: using pseudolikelihoods to infer potts models. *Physical Review E*, 87(1):012707, 2013.

[11] David T Jones, Daniel WA Buchan, Domenico Cozzetto, and Massimiliano Pontil. PSICOV: precise structural contact prediction using sparse inverse covariance estimation on large multiple sequence alignments. *Bioinformatics*, 28(2):184–190, 2012.

[12] David T Jones and Shaun M Kandathil. High precision in protein contact prediction using fully convolutional neural networks and minimal sequence features. *Bioinformatics*, 34(19):3308–3315, 2018.

[13] Sheng Wang, Siqi Sun, Zhen Li, Renyu Zhang, and Jinbo Xu. Accurate de novo prediction of protein contact map by ultra-deep learning model. *PLoS computational biology*, 13(1):e1005324, 2017.

[14] Jinbo Xu. Distance-based protein folding powered by deep learning. *Proceedings of the National Academy of Sciences*, 116(34):16856–16865, 2019.

[15] Jianyi Yang, Ivan Anishchenko, Hahnbeom Park, Zhenling Peng, Sergey Ovchinnikov, and David Baker. Improved protein structure prediction using predicted interresidue orientations. *Proceedings of the National Academy of Sciences*, 117(3):1496–1503, 2020.

[16] Shaun M Kandathil, Joe G Greener, Andy M Lau, and David T Jones. Deep learning-based prediction of protein structure using learned representations of multiple sequence alignments. *bioRxiv*, 2020.

[17] Claudio Mirabello and Björn Wallner. rawMSA: End-to-end deep learning using raw multiple sequence alignments. *PloS one*, 14(8):e0220182, 2019.

[18] Adam J Riesselman, John B Ingraham, and Debora S Marks. Deep generative models of genetic variation capture the effects of mutations. *Nature methods*, 15(10):816–822, 2018.

[19] Michael Remmert, Andreas Biegert, Andreas Hauser, and Johannes Söding. HHblits: lightning-fast iterative protein sequence searching by hmm-hmm alignment. *Nature methods*, 9(2):173–175, 2012.

[20] Julie D Thompson, Benjamin Linard, Odile Lecompte, and Olivier Poch. A comprehensive benchmark study of multiple sequence alignment methods: current challenges and future perspectives. *PloS one*, 6(3):e18093, 2011.

[21] Andriy Kryshtafovych, Torsten Schwede, Maya Topf, Krzysztof Fidelis, and John Moult. Critical assessment of methods of protein structure prediction (CASP)—Round XIII. *Proteins: Structure, Function, and Bioinformatics*, 87(12):1011–1020, 2019.

[22] Jürgen Haas, Alessandro Barbato, Dario Behringer, Gabriel Studer, Steven Roth, Martino Bertoni, Khaled Mostaguir, Rafal Gumienny, and Torsten Schwede. Continuous Automated Model EvaluatiOn (CAMEO) complementing the critical assessment of structure prediction in casp12. *Proteins: Structure, Function, and Bioinformatics*, 86:387–398, 2018.

[23] Sivaraman Balakrishnan, Hetunandan Kamisetty, Jaime G Carbonell, Su-In Lee, and Christopher James Langmead. Learning generative models for protein fold families. *Proteins: Structure, Function, and Bioinformatics*, 79(4):1061–1078, 2011.

[24] Stefan Seemayer, Markus Gruber, and Johannes Söding. CCMpred—fast and precise prediction of protein residue–residue contacts from correlated mutations. *Bioinformatics*, 30(21):3128–3130, 2014.

[25] John Jumper, R Evans, A Pritzel, T Green, M Figurnov, K Tunyasuvunakool, O Ronneberger, R Bates, A Zidek, A Bridgland, et al. High accuracy protein structure prediction using deep learning. *Fourteenth Critical Assessment of Techniques for Protein Structure Prediction (Abstract Book)*, 22:24, 2020.

[26] Ahmed Elnaggar, Michael Heinzinger, Christian Dallago, Ghalia Rihawi, Yu Wang, Llion Jones, Tom Gibbs, Tamas Feher, Christoph Angerer, Debsindhu Bhowmik, et al. ProtTrans: Towards cracking the language of life's code through self-supervised deep learning and high performance computing. *arXiv preprint arXiv:2007.06225*, 2020.

[27] Roshan Rao, Nicholas Bhattacharya, Neil Thomas, Yan Duan, Xi Chen, John Canny, Pieter Abbeel, and Yun S Song. Evaluating protein transfer learning with tape. *Advances in Neural Information Processing Systems*, 32:9689, 2019.

[28] Roshan Rao, Sergey Ovchinnikov, Joshua Meier, Alexander Rives, and Tom Sercu. Transformer protein language models are unsupervised structure learners. *bioRxiv*, 2020.

[29] Roshan Rao, Jason Liu, Robert Verkuil, Joshua Meier, John F Canny, Pieter Abbeel, Tom Sercu, and Alexander Rives. MSA transformer. *bioRxiv*, 2021.

[30] Alexander Rives, Joshua Meier, Tom Sercu, Siddharth Goyal, Zeming Lin, Jason Liu, Demi Guo, Myle Ott, C Lawrence Zitnick, Jerry Ma, et al. Biological structure and function emerge from scaling unsupervised learning to 250 million protein sequences. *Proceedings of the National Academy of Sciences*, 118(15), 2021.

[31] Pascal Sturmfels, Jesse Vig, Ali Madani, and Nazneen Fatema Rajani. Profile prediction: An alignment-based pre-training task for protein sequence models. *arXiv preprint arXiv:2012.00195*, 2020.

[32] Jan Chorowski, Dzmitry Bahdanau, Dmitriy Serdyuk, Kyunghyun Cho, and Yoshua Bengio. Attention-based models for speech recognition. *arXiv preprint arXiv:1506.07503*, 2015.

[33] Rohit Girdhar, Joao Carreira, Carl Doersch, and Andrew Zisserman. Video action transformer network. In *Proceedings of the IEEE/CVF Conference on Computer Vision and Pattern Recognition*, pages 244–253, 2019.

[34] Kai Han, Yunhe Wang, Hanting Chen, Xinghao Chen, Jianyuan Guo, Zhenhua Liu, Yehui Tang, An Xiao, Chunjing Xu, Yixing Xu, et al. A survey on visual transformer. *arXiv preprint arXiv:2012.12556*, 2020.

[35] Kaiming He, Xiangyu Zhang, Shaoqing Ren, and Jian Sun. Deep residual learning for image recognition. In *Proceedings of the IEEE conference on computer vision and pattern recognition*, pages 770–778, 2016.

[36] Jimmy Lei Ba, Jamie Ryan Kiros, and Geoffrey E Hinton. Layer normalization. *arXiv preprint arXiv:1607.06450*, 2016.

[37] Stephen K Burley, Helen M Berman, Charmi Bhikadiya, Chunxiao Bi, Li Chen, Luigi Di Costanzo, Cole Christie, Ken Dalenberg, Jose M Duarte, Shuchismita Dutta, et al. RCSB Protein Data Bank: biological macromolecular structures enabling research and education in fundamental biology, biomedicine, biotechnology and energy. *Nucleic acids research*, 47(D1):D464–D474, 2019.

[38] Diederik P Kingma and Jimmy Ba. Adam: A method for stochastic optimization. *arXiv preprint arXiv:1412.6980*, 2014.

[39] Qi Zhang, Jianwei Zhu, Fusong Ju, Lupeng Kong, Shiwei Sun, Wei-Mou Zheng, and Dongbo Bu. ISSEC: inferring contacts among protein secondary structure elements using deep object detection. *BMC bioinformatics*, 21(1):1–13, 2020.

[40] Zhiyong Wang and Jinbo Xu. Predicting protein contact map using evolutionary and physical constraints by integer programming. *Bioinformatics*, 29(13):i266–i273, 2013.

Checklist

1. For all authors...
   (a) Do the main claims made in the abstract and introduction accurately reflect the paper's contributions and scope? [Yes]
   (b) Did you describe the limitations of your work? [Yes] See Section 5.
   (c) Did you discuss any potential negative societal impacts of your work? [Yes] See Appendix.
   (d) Have you read the ethics review guidelines and ensured that your paper conforms to them? [Yes]
2. If you are including theoretical results...
   (a) Did you state the full set of assumptions of all theoretical results? [N/A]
   (b) Did you include complete proofs of all theoretical results? [N/A]
3. If you ran experiments...
   (a) Did you include the code, data, and instructions needed to reproduce the main experimental results (either in the supplemental material or as a URL)? [Yes] See Section 4.1 and Appendix.
   (b) Did you specify all the training details (e.g., data splits, hyperparameters, how they were chosen)? [Yes] See Section 4.1 and Appendix.
   (c) Did you report error bars (e.g., with respect to the random seed after running experiments multiple times)? [No] Though the local training process is stable, but our computational resources cannot afford to run dozens of experiments. Thus, we cannot provide reliable statistical results. To ensure the reproducibility of our method, we will submit our training code and model weights in the supplementary materials.
   (d) Did you include the total amount of compute and the type of resources used (e.g., type of GPUs, internal cluster, or cloud provider)? [Yes] See Section 4.1
4. If you are using existing assets (e.g., code, data, models) or curating/releasing new assets...
   (a) If your work uses existing assets, did you cite the creators? [Yes] See 4.1 and Appendix.
   (b) Did you mention the license of the assets? [Yes] See Appendix.
   (c) Did you include any new assets either in the supplemental material or as a URL? [No]
   (d) Did you discuss whether and how consent was obtained from people whose data you're using/curating? [N/A]
   (e) Did you discuss whether the data you are using/curating contains personally identifiable information or offensive content? [Yes] See Appendix.
5. If you used crowdsourcing or conducted research with human subjects...
   (a) Did you include the full text of instructions given to participants and screenshots, if applicable? [N/A]
   (b) Did you describe any potential participant risks, with links to Institutional Review Board (IRB) approvals, if applicable? [N/A]
   (c) Did you include the estimated hourly wage paid to participants and the total amount spent on participant compensation? [N/A]